

The mechanisms of strong-field control of chemical reactivity using tailored laser pulses

Noel P. Moore, Getahun M. Menkir, Alexei N. Markevitch, Paul Graham and Robert J. Levis

Department of Chemistry, Wayne State University, Detroit MI 48202, USA.

Control of chemical photoionization, dissociation, and rearrangement is demonstrated using tailored intense (10^{13} W cm^{-2}) laser pulses. The laser pulses are created using a closed-loop learning algorithm with the product distribution guiding the shape of the laser pulses. Control is demonstrated for the production of the acetone parent ion ($(\text{CH}_3)_2\text{CO}^+$), the competition of the products CH_3CO^+ vs. CH_3^+ during CH_3COCF_3 laser induced dissociation, and the rearrangement acetophenone ($\text{C}_6\text{H}_5\text{COCH}_3$) to produce $\text{C}_6\text{H}_5\text{CH}_3$ vs. $\text{C}_6\text{H}_5 + \text{CH}_3\text{CO}$. The generic nature of the technique is demonstrated and the fundamental underlying principles of such strong-field control experiments are considered.

Introduction

Controlling the electronic and nuclear dynamics of large polyatomic molecules requires, at the present time, tailored strong-field laser pulses (with intensity of approximately 10^{13} W cm^{-2}). Strong-field in this context implies the use of laser pulses where the maximum amplitude of the electric field ($\sim \text{V}\text{\AA}^{-1}$) rivals the fields binding valence electrons to nuclei (1). Tailored implies that the time-dependent electric field of the laser has been shaped (as described subsequently) to optimize a desired reaction channel (2). Controlling the outcome of matter-radiation coupling is desirable from both theoretical and practical points of view. From the theoretical perspective there are many new phenomena present in the interaction of intense laser pulses with molecules and furthermore it may be possible to unravel the details of a molecule's Hamiltonian from a family of control experiments (3) that would otherwise remain inaccessible using conventional methods. From the practical standpoint,

the control of chemical reactivity using strong-field optical pulses opens the twin horizons of combinatorial photochemistry and the development of an optical scalpel. The latter may now complement the methods of optical tweezers, cooling, and molasses. Computing a tailored optical field to control a chemical reaction from first principles is intractable for all but the simplest model systems because the molecular Hamiltonian is largely unknown. All is not lost for controlling chemical reactivity, as optimum solutions may be converged upon using closed-loop learning algorithms to selectively enhance one product channel at the expense of others (2). In this sense, the chemical control problem is like many other non-deterministic problems, such as those found in geometry optimization or in neural net design.

In the closed-loop paradigm for controlling chemical reactivity, one specifies a desired outcome for the interaction of the laser pulse and the molecule of interest. The laser pulse is then manipulated to produce a well-defined time-dependent electric field. This time-dependent electric field interacts with the molecule resulting in a series of photochemical/physical products. Measurement of the appropriateness of the product distribution with respect to a desired distribution allows the design of new pulses using an optimization algorithm. Closed-loop control with strong-field laser pulses is at the heart of all recent control experiments on complex systems. Such schemes have been used to control dissociation in inorganic (4) van der Waals (5), and now, organic molecules (6); chemical rearrangement channels (6); stimulated Raman emission from molecules (7); and high harmonic generation from atoms (8).

From a practical point of view, teaching lasers to control reaction dynamics (2) is now possible because of the convergence of three optical technologies. The first is the production of ultrashort laser pulses where a large number of discrete frequencies are coherently superimposed to produce a transform-limited pulse. Pulses on the order of 40 fs at 800 nm have tens of nanometers of frequency components that may be controlled to produce the desired laser pulse. The second technology is the use of spatial masking techniques (9) to selectively alter the phase and amplitude of the component frequencies of the transform limited pulse, thus producing a new laser pulse with a distinct time-dependent electric field. The third is the use of pulse amplification to increase the energy of the tailored laser to an intensity regime where chemical reactions may be induced (1). The control aspect then involves using a feedback-loop managed by a learning algorithm to converge upon the optimal mask to shape the time-dependent electric field to produce a desired reaction channel. The degree of control rests in part with the number of component frequencies (the bandwidth) available for tailoring the pulse. Even with the increased bandwidth of modern ultrafast laser systems, there are an insufficient number of frequencies to control complex chemical reactions, particularly if there are no resonant states within the range of the laser. This limitation may be circumvented by using strong-field laser pulses which serve to “artificially” increase the excitation bandwidth as described (10).

We demonstrate control of photoionization, dissociation and rearrangement using a strong-field, ultrafast closed-loop excitation scheme. We show that control of the photoionization/dissociation distribution is possible both by altering the intensity and/or pulse duration of the near transform limited pulse, as well as by controlling the detailed temporal profile of the intensity of the pulse. Examples of each of these control methods are presented. Finally the underlying mechanisms of multiphoton excitation, transient shifting of intermediate states and lifetime broadening of eigenstates are discussed to explain this novel control paradigm.

Experimental

The oscillator pulse is an 86 MHz pulse train of 20 fs pulses centered at 800 nm. The pulses are stretched to 100 ps using two gratings. The stretched pulses are then amplified to 3 mJ in a 10 Hz regenerative amplifier and are compressed to 80 fs using a dual grating system. Pulse shaping to produce the time-dependent electric fields is achieved by means of a spatial light modulator (SLM) placed at the Fourier plane of the pulse stretcher, as shown in Figure 1. The SLM consists of two registered linear arrays containing 128 pixels (liquid crystals) each. In the present work, groups of 16 pixels are linked together to

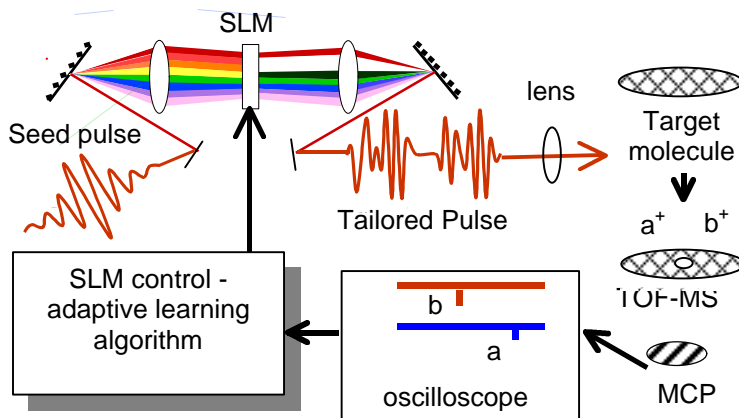


Figure 1. A schematic of the optical layout used to produce the tailored, strong-field laser pulses.

create a genome with 2×8 variable regions or genes. Each variable region is biased to a voltage that controls the relative phase and amplitude of the frequency components travelling through each region. The tailored laser pulses are focused to a $100 \mu\text{m}$ diameter spot in the analysis chamber using a 20 cm lens. Spatial inhomogeneities in the laser focal volume present no significant problem as the genetic algorithm can cope with this instability (10). Target molecules are thermalized in vacuum to a pressure of $\sim 10^{-6}$ torr. The outcome of

the interaction of the tailored pulses with the target molecule is monitored by means of time-of-flight mass spectroscopy.

A genetic algorithm (11) is employed to iteratively converge the evolving laser pulses to the optimal pulse for controlling the reaction dynamics as desired. Concepts of evolutionary biology are applicable in development of efficient genetic algorithms. Individual pulses can be evaluated in terms of their ‘fitness,’ which is a quantitative measure of how close an outcome is to the desired target. This may be written as:

$$J=(O - O^*)^2 \quad (1)$$

where J is the cost, O is the observable and O^* is the desired target for the observable. The concept is to minimize the cost by finding the time-dependent electric field, $\epsilon(t)$, that optimally matches O to O^* . A scheme that allows only the fittest members (laser pulse shapes or $\epsilon(t)$) of a population to survive and create new pulses will eventually converge on an optimal control genome. The details of the algorithm are specific to each objective posed. In our experiments, a population of 40 distinct members (laser fields) was propagated to find the optimal pulse. Despite the large search space, an optimum solution can be converged upon rapidly by judicious choice of optimization algorithms (12). In subsequent generations new members are generated after proportional selection by random crossover and a mutation rate of 6% per individual, per generation.

In an effort to determine the viability of the method as a tool for controlling photoprocesses, reference experiments were performed. The target molecules were exposed to the unshaped reference pulse (80 fs) and the mass spectra were recorded as a function of laser intensity. The laser intensity was adjusted by placing glass slides (200 μm thick) with known transmission characteristics into the beam path. The use of such slides was not found to affect the group velocity dispersion of the pulse in any significant manner, but reduced pulse energy by approximately 7% per slide. The target molecules were also studied as a function of laser pulse duration by linearly chirping the pulses. The reference experiments serve to give some knowledge of most likely reaction pathways for a given molecule under the influence of the intense 800 nm \pm 10 nm laser pulses.

Results

An example of pulse energy and pulse duration control of the photoionization and dissociation processes is shown in Figure 2 for the molecule p-nitroaniline (PNA). The pulse intensity was varied from 2.5-15 $\times 10^{13}$ W cm^{-2} in Figure 2A by varying the laser from 0.1 to 0.6 mJ per pulse with pulse duration held constant at 80 fs. An alternative method to alter the laser intensity was to maintain constant pulse energy while increasing the laser pulse duration. The duration can be increased in our apparatus by altering the grating separation in the compressor. The intensity is varied in Figure 2B from 0.3-15 $\times 10^{13}$ W cm^{-2} by altering the pulse duration while holding the energy constant at 0.6 mJ per pulse.

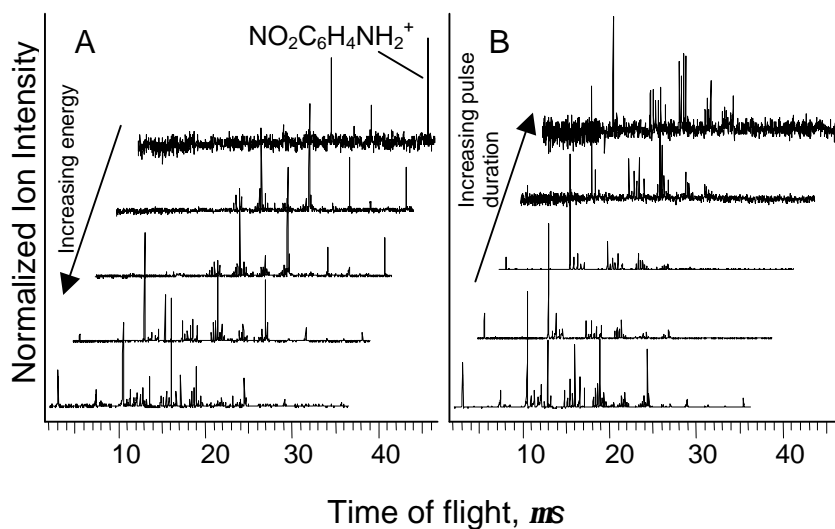


Figure 2. Time-of-flight ion spectra of p-nitroaniline subjected to 790 nm laser pulses. In Figure 2A the pulse energy was varied from 0.60 to 0.10 mJ/pulse, the pulse duration was 80 fs. In Figure 2B the pulse duration was varied from 100 fs to 5 ps, the pulse energy was 0.60 mJ/pulse.

The major trend observed in Figure 2A is the increase in the degree of fragmentation with increasing laser pulse energy. The molecular ion and large ion fragments are the major species observed at low laser intensity. If the laser pulse duration was increased while keeping the pulse energy constant, a significant degree of fragmentation was observed at all pulse durations, including at the laser intensity corresponding to the ion appearance threshold. Thus at the same laser intensity, as shown in the top two traces in Figure 2, we observe limited fragmentation for the transform limited pulse and considerable fragmentation for the stretched pulse. This experiment demonstrates that a degree of control over various fragmentation pathways can be achieved by simply varying laser pulse energy and/or duration.

Pulse shaping was investigated to attempt more sophisticated control over the photoionization and fragmentation distribution of the molecule acetone, $(\text{CH}_3)_2\text{CO}$. Figure 3 displays the results for the case where optimization of the parent peak in the mass spectrum of acetone was the specified goal in the control algorithm. Figure 3A shows two of the mass spectra taken as a function of generation number during the optimization. These spectra are representative of the 40 members of a given generation. The control algorithm was able to substantially increase molecular ion peak from a minimal level at the start of the experiment to being an easily detectable ion signal within a few generations. Subsequent increase in the parent signal was not found after the 13th generation despite the action of the genetic operators. Fluctuations in the relative abundance

of the parent peak after the 13th generation are expected due to the algorithm's attempts to improve upon the trial field by crossover and mutation. These fluctuations are local and do not affect the globally converged solution. The relative signal of parent peak as a function of generation number is shown in Figure 3B. In accord with the results of the survey experiments on acetone, the algorithm converged on a near transform limited pulse with which to maximize the parent signal. This simple experiment shows that it is possible to use shaped pulses to alter the appearance of the mass spectral distribution not only in terms of overall ion intensity, but also in terms of the fragmentation distribution.

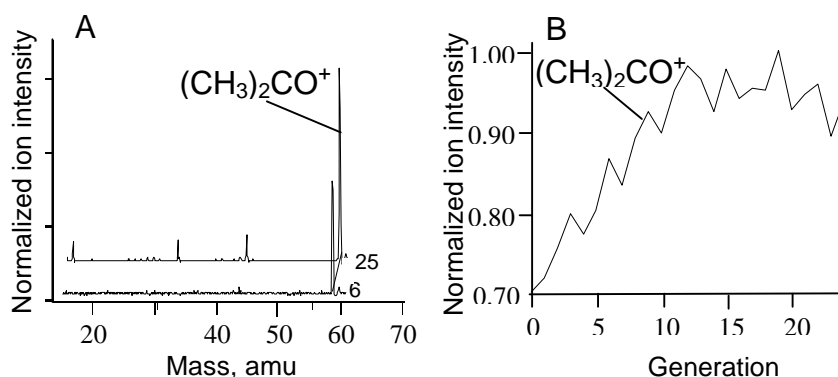


Figure 3. A) The mass spectra as a function of generation during the optimization of the laser pulse; B) The optimized acetone ion signal as a function of generation.

The survey experiments for acetone reveal that the optimum pulse for parent production is one that increases the laser intensity with a transform limited pulse. This optimal pulse is not surprising because increasing the laser pulse duration typically leads to increased dissociative ionization. Thus, the control exhibited in this case can be described as *trivial*, as there is no specificity to the molecular Hamiltonian incorporated into the optimum solution. *Non-trivial* control schemes depend on the evolution of the molecular Hamiltonian under the influence of the radiation and are hence molecule-specific.

Comparing the yields of two different ions from the simple intensity and pulse duration reference experiments to the yields from the genetic algorithm experiment may reveal whether the control exerted is trivial or non-trivial. Figure 4 presents the results from a closed-loop optimization on the molecule trifluoroacetone, CH_3COCF_3 , where maximization of the ratio $\text{CH}_3^+/\text{CH}_3\text{CO}^+$ was specified. In these experiments the ion signals and ratios are normalized to unity at generation zero as the experiment starts with a randomly generated optical field. At the start of each optimization experiment, the absolute yields of the CH_3^+ and CH_3CO^+ ions were within a factor of two of each other. In this experiment the largest ratio between the two ions was 1.8. The increase in the

ratio was mainly due to a significant increase in CH_3^+ yield, however both ions increased in overall intensity. Reference experiments reveal no trend in the $\text{CH}_3^+/\text{CH}_3\text{CO}^+$ ratio as a function of laser energy. Furthermore, the ratio decreases with increasing pulse duration, opposite to that shown in Figure 4. The trends in the reference experiments suggest that that non-trivial control is exerted in this case.

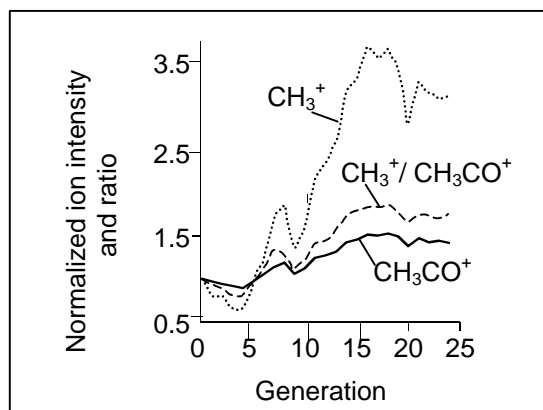


Figure 4. The relative intensity for CH_3^+ , CH_3CO^+ , ion formation from CH_3COCF_3 , and the ratio of ions as a function of generation in the optimization algorithm. All curves are normalized to unity at the initial generation for this plot.

To eliminate the possibility that the non-trivial control observed was influenced by the choice of functional groups in trifluoroacetone, we attempted control on the photochemical reaction dynamics of the molecule acetophenone, $\text{C}_6\text{H}_5\text{COCH}_3$. The mass spectrum for acetophenone exposed to the transform limited pulse is presented in Figure 5A. Observable are peaks corresponding to laser-induced cleavage of the methyl and phenyl species from the parent molecule. A previous investigation (6) detailed control of the branching ratios for cleavage of the phenyl and methyl species from the acetone precursor. Control over the branching ratios of a factor of four was measured. The corresponding reference experiments suggested that the control fell into the nontrivial class, similar control could not be achieved by varying either the laser pulse duration or the laser energy.

In addition to expected peaks in the mass spectrum, a peak exists at $m/z = 92$ amu. This peak corresponds to toluene, $\text{C}_6\text{H}_5\text{CH}_3$, as confirmed by complementary investigations on the deuterated acetophenone $\text{C}_6\text{H}_5\text{COCD}_3$. The toluene is a product of field-induced molecular rearrangement of the precursor acetophenone molecule. To test whether control is possible we first attempted to minimize the toluene yield by maximizing the ratio $\text{C}_6\text{H}_5^+/\text{C}_6\text{H}_5\text{CH}_3^+$. This optimization goal seeks to enhance phenyl group cleavage representing dissociation in comparison to the rearrangement channel. This ratio of the averages is plotted as a function of generation number in Figure 5B. The yield reaches a maximum of a factor of 1.9 at generation 15. We next attempted to maximize the rearrangement of the toluene product in preference to the phenyl

dissociation product, thereby maximizing the ratio $C_6H_5CH_3^+/C_6H_5^+$. The method manages to increase the ratio to 2.5 by holding the $C_6H_5CH_3^+$ constant and suppressing the $C_6H_5^+$ peak. This optimization as a function of generation

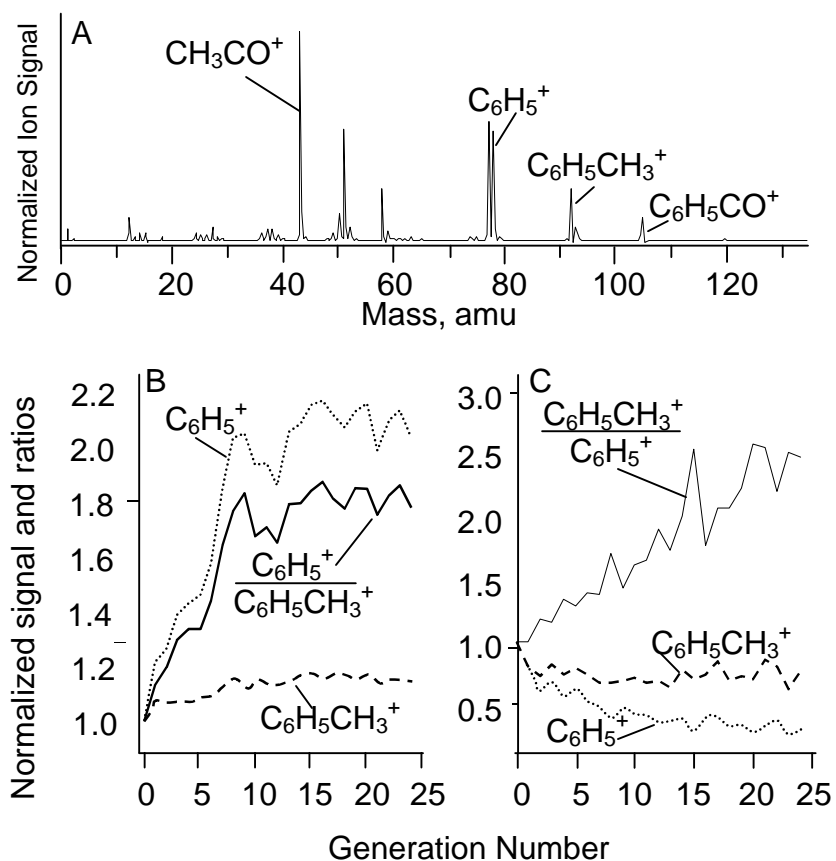


Figure 5. A, The strong-field mass spectrum for acetophenone; B, the learning curve and ion yields when minimization of the toluene:phenyl yield is specified; C, the learning curve when maximization of the toluene:phenyl yield is specified.

number is shown in Figure 5C. In both control optimizations, the toluene ($C_6H_5CH_3^+$) signal remains approximately constant while the algorithm adjusts the phenyl ion ($C_6H_5^+$) yield. Clearly both pathways compete with each other starting from an excited parent molecule. However, the genetic algorithm can control the relative abundance of each pathway. The tailored pulses used in Figure 5B and C can change the $C_6H_5^+/C_6H_5CH_3^+$ ratio over a dynamic range of ~5. In the case of trivial control, it is unlikely that one ion yield remain

constant while another would be free to fluctuate in intensity. Finally, absolute ion yield is seen to increase monotonically with decreasing pulse intensity or increasing pulse duration. Such correlation is not evident in the results of the control experiment shown in Figure 5.

Discussion

The results shown in Figure 2 demonstrate that control of the ion intensities in the mass spectrum of parinitroaniline can be accomplished using intensity and pulse duration variation in a transform limited pulse of high intensity ($\sim 10^{13}$ Wcm⁻²). The degree of control is substantial and is indicative of photoinduced nuclear excitation of the molecule under the given excitation conditions. The pulse shaping experiments described in this work (see Figures 3 4 and 5) and in previous investigations (4-5) strongly suggest that control over the photo-induced dissociation, and now rearrangement of molecules, can be accomplished using tailored laser pulses in the strong-field regime. All of the control systems studied previously (from simple liquids, to inorganics to and array of organics) were excited using short duration laser pulses of with wavelengths centered in the region of 800nm. Since none of the systems have even vaguely similar absorption profiles, one may ask the question as to what the control mechanism is? The solution to this question, we propose, is a combination of strong-field excitation processes. In the strong-field regime multiphoton absorption of up to 50 photons may occur. In addition, field-induced shifts of molecular eigenstates (13) allows a greater degree of control over reaction dynamics. Finally, with the intense excitation scheme there is also a lifetime broadening mechanism that increases the “bandwidth” of the overall excitation scheme. The wide range of bond selective chemistry displayed using intense, near-infrared radiation of femtosecond duration with the rather narrow bandwidth (~ 0.1 eV) is not surprising in light of the highly non-linear multiphoton excitation coupled with the marked effects of the electric field of the radiation on the energy levels of the molecule.

To understand the nature of strong-field excitation for control purposes it is useful to realize that field-induced electronic motion during the pulse essentially determines the nuclear motion after the pulse. This is because the laser pulse has short duration, on the order of a picosecond or less, while nuclear resulting in dissociation or rearrangement of large molecules typically requires longer time scales. All of the electronic states available in a polyatomic molecule form the basis set in which an arbitrary 3-dimensional motion of electrons inside the potential energy surface can be expressed (14). To be able to shape the 3-dimensional motion of the electrons inside electrostatic surface during a laser pulse in a specific way, a large number of electronically excited states must be excited and combined with a definite phase relationship.

A significant amount of experimental data (16-20) suggests that polyatomic molecules subjected to a dynamic strong-field can undergo multiple electronic excitations. The strong-field multi-electron excitations are the initial stage of highly inelastic (diabatic) laser/molecule coupling which may result in prolific nuclear motion, extensive fragmentation and large kinetic energy release of the fragment ions. It is encouraging that a large number of coupling channels can be accessed simultaneously in the strong-field regime as shown, as shown for instance in Figures 2 and 5.

Studying the coupling of molecules with unshaped strong-field laser pulses may reveal some rules of thumb for control experiments in the strong-field regime. Of particular interest to control experiments is the total amount of energy deposited during the laser/molecule interaction and the subsequent partitioning of the deposited energy among product channels. Recent data on kinetic energy release of H^+ fragment ions resulting from dissociative ionization of polyaromatic hydrocarbons demonstrate that H^+ ions with energies up to 60 eV are formed (17). This implies that up to 40 photons may be deposited in a single dissociative coupling channel. The large number of photons available for excitation is presumably responsible for the fact that a wide variety of molecules have been excited, ionized and detected using femtosecond duration radiation centered at 800 nm. Such highly nonlinear excitation must also play an enabling role in the mechanism of strong-field control. Unlike linear excitation schemes, strong-field excitation may employ a wide array of excited states to construct the most appropriate wave function for the desired final product states. Thus, the fact that a series molecules have (or do not have) similar absorption spectra has little to do with the degree of intense laser-molecule coupling.

Further evidence that a variety of coupling channels may be accessed simultaneously in the strong-field regime is found in photoelectron kinetic energy measurements of polyatomic molecules (15). The dynamics that determine the final product distribution are controlled by the mechanisms of energy coupling and subsequent partitioning. Despite the wealth of experimental (16, 17, 18, 19, 20) and computational studies (21, 22, 23, 24) probing strong-field excitation of molecules, the topic is still far from well-understood.

Insight into the interaction of intense lasers on atomic and molecular energy levels has been gained by investigating electron dynamics, both theoretically and experimentally (25). The strong-field photoelectron spectroscopy of acetylene (18), for instance, revealed the presence of above threshold ionization. This process involves signatures in the photoelectron spectrum resulting from, in this case, up to eight photons being absorbed in addition to that required to overcome the ionization potential. Such measurements demonstrate that even for a small molecules such as acetylene, at least 15 photons may be involved in the strong-field excitation event. The assignment of the features observed in these measurements revealed that the excited states of the molecule shifted up to 5 eV in the presence of the field. The myriad of strong-field phenomena revealed in photoelectron spectra underpin

the wide range of coupling mechanisms which are central to exerting non-trivial control over chemical reactivity.

Further effects of the strong radiation fields on the molecular Hamiltonian are highlighted in a study of the photoelectron spectroscopy (26) of the molecules benzene (C_6H_6), naphthalene ($C_{10}H_8$) and anthracene ($C_{14}H_{10}$) at the single laser intensity, $4.0 \times 10^{13} W cm^{-2}$. The measurements revealed an apparent decrease in the resolution of the photoelectron peaks with increasing molecular size. The smallest molecule, benzene, displayed a discrete spectrum of photoelectron peaks. Naphthalene displayed a series of discrete photoelectron peaks superimposed upon a broad, featureless distribution of electron kinetic energies. Anthracene, the largest molecule displayed an unstructured photoelectron kinetic energy spectrum. The modal and maximum kinetic energies recorded were seen to increase with molecular size. The data was interpreted in light of a *structure-based* model (16) that considers aspects of the electrostatic potential energy surface and was used to infer an evolution from a regime dominated by multiphoton ionization (MPI) for benzene to a regime dominated by field-ionization for anthracene. Such results clearly demonstrate that the degree of coupling increases in the strong-field limit as the characteristic length of the molecule increases.

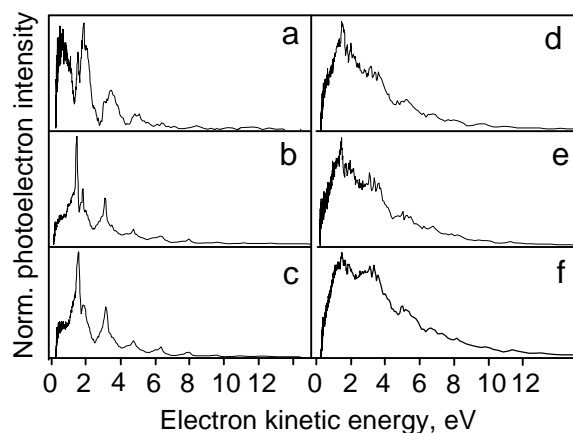


Figure 6. The photoelectron spectra for acetylene excited using 130 fs duration pulses of 800nm radiation. The intensity of the radiation is: a, $5.7 \times 10^{13} W cm^{-2}$; b, $6.9 \times 10^{13} W cm^{-2}$; c, $8.6 \times 10^{13} W cm^{-2}$; d, $10^{13} W cm^{-2}$; e, $1.1 \times 10^{13} W cm^{-2}$; f, $1.4 \times 10^{13} W cm^{-2}$.

The loss of discrete features for larger characteristic lengths in the benzene, naphthalene, anthracene series is proposed to be due to a lifetime broadening mechanism. To test this hypothesis the photoelectron spectra for naphthalene were measured for a range of laser intensities (13). In the context of the structure-based, tunnel ionization model as the intensity is increased the uncertainty in state lifetime should decrease. The measured spectra evolved from a series of assignable peaks at the lower intensities to a broad, featureless distribution of electron kinetic energies at higher intensity. The modal and maximum kinetic energies recorded were noted to increase as the laser intensity increased. Similar trends have been observed for benzene (15) and anthracene

suggesting the existence of a generic field-induced mechanism for broadening of molecular eigenstates.

Figure 6 presents the strong-field photoelectron spectra of acetylene, C_2H_2 (panels a-f) and benzene. The trend observed is qualitatively similar to that of the naphthalene data reported previously (13). The spectra evolve from a structured photoelectron spectrum at the lower intensities toward a broader, less-featured distribution of kinetic energies as the laser intensity is increased. This suggests that even a small molecule, such as acetylene may undergo the lifetime broadening mechanism.

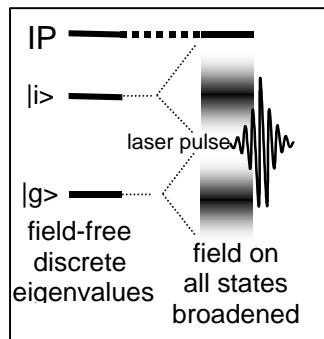


Figure 7. A schematic of the field induced broadening that contributes to the effective bandwidth of the laser.

The structure-based model supports the inherently intuitive picture that field-ionization becomes easier as the laser intensity increases. The increasing rate of field ionization is key to understanding the loss of structure in the photoelectron spectra as the laser intensity is increased. If field-ionization is enhanced at higher laser intensity, eigenstate population is likely to decrease accordingly. Thus field ionization and any other events that cause eigenstate population decay will shorten the lifetime of such eigenstates. As the lifetime of a state is shortened, the uncertainty in the lifetime is also shortened. From the Heisenberg uncertainty principle ($\Delta t \cdot \Delta E \geq \hbar$, in atomic units), it is clear that the eigenvalue uncertainty is equal to or greater than the inverse of the uncertainty in the eigenstate lifetime. If we assume that a state can survive no longer than the time required to field ionize, we can equate the uncertainty in state lifetime with the field-ionization lifetime. This is because the state lifetime should have an upper bound of the field-ionization lifetime. Thus a broadening of the photoelectron peaks with increasing laser intensity is anticipated because the ionization probability increases with laser intensity. The corresponding broadening of intermediate states is illustrated in Figure 7. Calculation of the ionization probability for the molecule naphthalene at an intensity near $5 \times 10^{13} \text{ W cm}^{-2}$ suggests that the ionization rates will result in lifetime broadening on the order of 5 eV. The broadening calculated increased with the laser intensity and was on the same order of magnitude to that measured experimentally.

The field-induced broadening mechanism has been demonstrated in various molecules and seems to be a generic phenomenon in strong-field excitation process. While, field-induced eigenstate broadening mechanism might be viewed as a limitation for spectroscopic investigations, for strong-field optical control, the broadening mechanism might be viewed favorably as adding additional bandwidth to the nominally narrow bandwidth femtosecond laser. Such eigenstate broadening in combination with nonlinear (multiphoton) absorption in the strong-field regime should work in tandem to provide diverse coupling schemes. Non-trivial strong-field control can only be exerted if the full dynamic capabilities of a molecule are employed. The strong-field, time-dependent laser pulse appears to have the ability to create resonances as needed, and therefore circumvents the spectral limitations present in virtually all weak field excitation schemes.

Conclusions

We have shown control of reaction dynamics for p-nitrotoluene using the variables of intensity and pulse duration and in a series of ketones using tailored strong-field pulses under closed-loop control. We have presented data that shows control in both trivial and non-trivial schemes. The observations are discussed within the context of a multiphoton picture that includes transient shifting of intermediate states as well as lifetime broadening. Within these strong-field processes the range of coupling and partitioning channels is large and it is anticipated that laser-induced control of nuclear motion in the strong-field regime will be a viable tool for guiding chemical reactivity.

Acknowledgements

The authors would like to acknowledge the support of the Office of Naval Research and the National Science Foundation for this work.

References

-
- 1 DeWitt, M. J.; Levis, R.J. *J. Chem. Phys.* **1995**, *102*, 8670.
 - 2 Judson, J.S.; Rabitz, H. R. *Phys. Rev. Lett.* **1992**, *68*, 1500.
 - 3 Rabitz, H.R. *et al. Science.* **2000**, *288*, 824.
 - 4 Assion, A, *et al. Science* **1998**, *282*, 919.
 - 5 Daniel, C. *et al. Chem. Phys.* *2001 in press.*
 - 6 Levis, R. J.; Menkir, G. M.; Rabitz, H. R. *Science in press.*
 - 7 Weinacht, T. C.; Ahn, J.; Bucksbaum, P. H. *Nature*, **1999**, *397*, 233.
 - 8 Bartels, R.; Backus, S.; Zeek, E.; Murnane, M. M.; Kaptyen, H. C. *Nature* **2000**, *406*, 164.
 - 9 Weiner A. M.; Leaird, D. E.; Patel, J. S.; Wullert, J. R. *IEEE J. Quant. Electron.* **1992**, *28*, 908.
 - 10 Sunderman, E.; Rabitz, H. R.; De Vivie-Riedle, R. *Phys. Rev. A.* **2000**, 6201
 - 11 *Genetic Algorithms in Search optimization and Machine Learning*, Goldberg, D. Addison Wesley, Reading, Mass, 1989.
 - 12 Demiralp, M.; Rabitz, H. R.; *Phys. Rev. A.* **1993**, *47*, 809.
 - 13 Moore, N. P., Levis, R. J., *J. Chem. Phys. Submitted.*
 - 14 Mukamel S.; Tretiak S.; Wagersreiter T.; Chernyak V. *Science* **1997**, *277* , 781.
 - 15 Moore, N. P.; Markevitch, A. N.; Levis, R. J. *in prep.*
 - 16 DeWitt, M. J.; Levis, R. J., *J. Phys. Chem. A* **1999**, *103*, 6493.
 - 17 Markevitch, A. N.; Moore, N. P.; Levis, R. J. *Chem. Phys. in press.*
 - 18 Moore, N. P.; Levis, R. J. *J. Chem. Phys.* **2000**, *112*, 1316.
 - 19 Moore, N. P.; Levis, R. J. *J. Chem. Phys. submitted*
 - 20 Lezius, M.; Blanchet, V.; Rayner, D. M.; Villeneuve, D. M.; Stolow, A.; Ivanov, M. Yu. *Phys. Rev. Lett.* **2000**, *86*, 51.

 - 21 Corkum, P. B.; Burnett, N. H.; Brunel, F. *Phys. Rev. Lett.* **1989**, *62*, 1259.
 - 22 Corkum, P. B. *Phys. Rev. Lett.* **1993**, *71*, 1993.
 - 23 Walker, B.; Sheehy, B.; Kulander, K. C.; DiMauro, L. F. *Phys. Rev. Lett.* **1996**, *77*, 5031.

 - 24 Hankin, S. M.; Villeneuve, D. M.; Corkum, P. B.; Rayner, D. M. *Phys. Rev. Lett.* **2000**, *84*, 5082.

 - 25 Blanchet, V. *et al. Faraday Discussions*, **2000**, *115*, 33.
 - 26 DeWitt, M.J. and Levis, R. J., *Phys. Rev. Lett.* **1998**, *81*, 5101.